GRAPHICAL DISPLAY FOR ANNUAL CLIMATE-BASED DAYLIGHT SIMULATION

Siân Kleindienst[1], Magali Bodart[2], Marilyne Andersen[1]

[1]Building Technology Program, Dept of Architecture, Massachusetts Institute of Technology, Cambridge, USA
[2] Architecture et Climat, Université Catholique de Louvain, Louvain-la-Neuve, Belgium

ABSTRACT

Due to daylight variability, a design cannot be thoroughly assessed using single-moment simulations, which is why we need dynamic performance metrics like Daylight Autonomy and Useful Daylight Illuminance. Going one step further, the annual variation in performance (condensed to a percentage by DA and UDI) is also valuable information, as is the ability to link this data to spatial visualizations and renderings. The challenge, therefore, is to provide the information necessary to early design decision-making in a manageable form, while retaining both the continuity of annual data. This paper introduces a simplification method based on splitting the year into weather-averaged periods, which are simulated using Perez's ASRC-CIE sky model while sun penetration data is provided at greater resolution. The graphical output, in "Temporal Map" format, is shown to be visually and numerically comparable to reference case maps created using detailed illuminance data generated by Daysim.

INTRODUCTION

The quality of daylighting designs depend heavily on the solar altitude, the weather, and other time-dependant environmental factors. Yet very few existing tools provide the user with some understanding of the annual performance of a daylighting design, and similarly few lighting metrics focus on this temporal aspect of light measurement. S.P.O.T. [1] and Daysim [2] are two exceptions to the rule which provide these capabilities through calculations of *Daylight Autonomy* (DA) [2], a metric which provides the percentage of annual occupancy hours above a given illuminance benchmark. A recent collaborative paper, by both the creators of DA and of the similar Useful Daylight Illuminance (UDI) metric [3], outlines the benefits and limitations of analyses performed using dynamic daylighting metrics [4].

For the sake of readability, it is impossible to show all available data in a single graph. DA and UDI choose to sacrifice an understanding of the time-based performance variability in favor of retaining spatial performance variability. On the other hand, the "Temporal Map" graphical format suggested by Mardaljevic [5] displays data on a surface map whose axes represent the hours of the day and the days of the year; this retains the temporal variability of performance in a very dense format. The combination of these two approaches would produce a highly detailed analysis of the performance of a space, showing how performance varies both over space and over time. Beyond the practical implications of this approach in terms of computation, the greatest challenge involved in producing such an immense data set is to make sure it can be easily absorbed and interpreted by a designer.

Indeed, while the number annual periods for which full simulations must be done has an effect on the program's simulation time, it also has a less obvious, but important, effect on the readability of the graphical output. A low temporal resolution of simulations might short-change the variability of sky conditions; but similarly, a very high resolution might require too much mental processing by the user to be quickly synthesized and translated into design changes. Because of this, information pre-processing becomes a precious advantage – one which goes beyond interactivity and calculation time concerns. In preparing data for quicker analysis, however, care must be taken to ensure that any information critical to inform design in its early stages is not lost through this process.

This paper describes how a simplified annual data set, created by splitting the year into a relatively small number of periods of "similar moments" and using the ASRC-CIE sky model [6], can produce temporal maps which are visually, and even numerically, comparable to detailed reference case maps created using Daysim.

METHODOLOGY

In dividing the year into "similar" periods that will ultimately be represented by single points on a temporal map, the most important consideration is to ensure that these periods include a range of conditions as limited as possible. The sun should be at

approximately the same position in the sky, as only one sun position will represent the whole period, and the weather should be reasonably stable – both of which require that a group of moments be similar in both time of day and time of year.

For the test cases below, the year was divided into 56 periods: the day is divided into 7 intervals, and the year into 8. All times of day are in solar time, and since noon is an important solar day benchmark, it was decided preferable to divide the day into an odd number of intervals. The seven daily intervals are spaced equally from sunrise to sunset, so that longer days are not over-represented. The year is divided by an even number, so that the solstices may serve as interval limits. This is so that the sun positions, determined by the day and time central to each interval, represent average, not extreme angles. This method of division results in 28 unique sun positions at 56 times of year, as shown in figure 1. This method provides adequate temporal resolution for data like general illuminance but not for irect sun penetration effects.

The ASRC/CIE sky model, developed by Perez, is the one used in this paper. It integrates the four standard CIE sky models into one angular distribution of sky luminance – the standard CIE overcast sky (Hopkins), the CIE averaged intermediate sky (Nakamura), the standard CIE clear sky, and a high turbidity formulation of the latter (CIE clear sky for polluted atmosphere) [7].

This sky model has been validated for diverse climate and sky zones (sun proximity) [6,8] and compared with several other models. Comparison results vary from one study to another, but the ASRC model always gives good results, sometimes even better results than the more complex "all-weather sky model", also developed by Perez [9] and validated with several other models [6,8,10]. According to Perez [6], the good performance of the ASRC model is due to the two-fold parameterization of insolation conditions which help differentiate between sky clearness and sky brightness. The ASRC-CIE model was validated by Littlefair against the extensive BRE sky-luminance distribution dataset [8]. It exceeded most other sky models, including the Perez All-Weather model, in accuracy and was declared most likely to be adaptable to a wide range of climate zones.

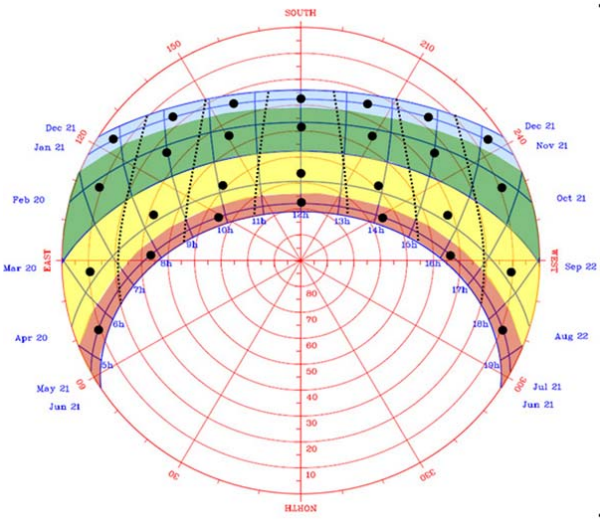

Figure 1: Sun course diagram overlaid with the 56 periods (28 unique sun positions). The colored bands show the division of the year, and the dotted lines show the division of the day.

The ASRC-CIE model was deemed the most appropriate sky model for use in time-based processing, because it is not only accurate, but conducive to averaging many skies in a realistic way. Given typical meteorological data for all time within a certain range of days and hours, one can find an average horizontal illuminance separately for each of the major sky types (clear, clear-turbid, intermediate, and overcast) and the percent chance of that sky type occurring within that period. Using these averaged values and weights, one can create four realistic, instantaneous sky maps which still represent the entire period in question. One could not get the same effect using the All-Weather Perez model, for example, because averaging data from different types of skies might result in one sky map which is both impossible and unrepresentative of any sky that might occur within that time frame.

The governing equation of the ASRC-CIE model is the following:

$$E_{vc} = b_c E_{vc.cie.c} + b_{ct} E_{vc.cie.ct} + b_i E_{vc.cie.i} + b_o E_{vc.cie.o} \quad (1)$$

where E_{vc} is the illuminance at a sensor point and $E_{vc.cie.c}$, $E_{vc.cie.ct}$, $E_{vc.cie.i}$ and $E_{vc.cie.o}$ are, respectively, the illuminances at that sensor point under a standard CIE clear sky, a standard CIE clear turbid sky, a CIE intermediate sky and a CIE overcast sky.

The weighting factors b_c, b_{ct}, b_i, b_o, which were adopted by Perez in 1992, depend on the sky clearness ε and brightness Δ [6]. The ε and Δ are calculated using the horizontal diffuse irradiance, the normal incident irradiance, and the solar zenith angle. For any given ε and Δ, two of the four skies are selected depending on the prevailing value of sky clearness ε, and are then assigned b_j coefficients, or the probability of each sky occurring.

In short, this temporally-based averaging method divides the year into 56 periods. For each period, the

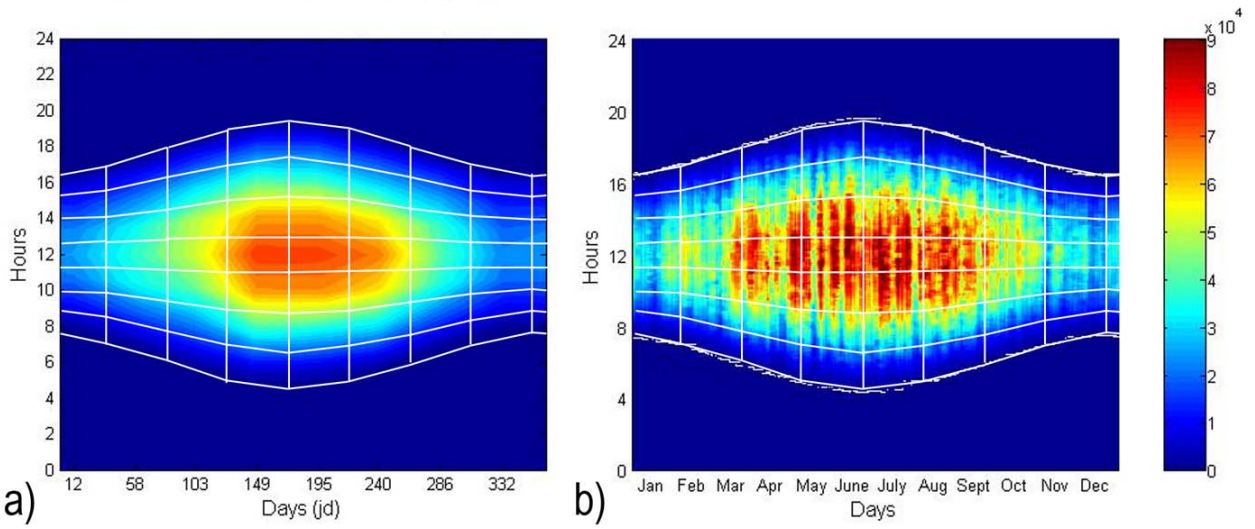

Figure 2: Comparison of temporal maps: Temporal averaging approach (a) versus the corresponding reference case created using Daysim data (b). Overlaid on both maps is the division of the year into 56 periods, which is also the physical boundary of pixel areas analyzed for average value similarity. This particular pair of maps represents the illuminances gathered by the unobstructed horizontal sensor in a Boston environment.

average b_j coefficients are calculated, together with the average diffuse horizontal illuminances. Point illuminance values are then calculated using the central sun position for the considered period, each of the four CIE sky types, and the weighted sum is calculated using the average b_c, b_{ct}, b_i and b_o coefficients. The one instance in which this method failed was for intermediate skies with sun altitudes greater than 80°. Since the failure was caused by the inaccuracy of the CIE intermediate sky model at high sun altitudes [8], these few simulations are replaced by All-Weather model simulations where ε is set equal to 1.35.

The previous paragraphs describe the process used for dividing the year into 56 groups of similar moments, and how one may arrive at a single representative illuminance value for the whole period in question. What remains is to put this averaged data into an intuitive graphical form in order to understand how the illuminance level responds to hourly and yearly changes in weather and sun position.

In 2003, Mardaljevic introduced the concepts of Spatio-Temporal Irradiation Maps (STIMAPs) – surface graphs following the year on the x-axis and the day on the y-axis [5]. Other applications of the basic concept behind STIMAPs can be found in ECOTECT for the display of ventilation- and solar-thermal gains [11], or in the SPOT! program for direct shadows [12].

Coupled with spatial renderings, temporal maps are an intuitive and powerful way in which to view an entire year's worth of daylighting analysis in one glance. Figure 2 shows the authors' adaptation of the "Temporal Map" concept with the corresponding reference case graphs. Figure 2a is a contour graph of the 56 data points. Points were added at sunrise and sunset on each of the 8 days where the illuminance was set to zero, in order to keep the daily extreme contours from falling off to quickly. Figure 2b is a surface graph representing the illuminances calculated by DAYSIM. It is composed of 105,120 data points (one for every five minute interval during the year) and is thus dense enough to need no contour interpolation between data points. Despite the obvious detail reduction from the Daysim surface maps to the averaged contour graphs, the latter approach doesn't seem to hide most important features while making general trends in performance clearer. All graphs in this paper were produced using MATLAB, and illuminance calculations for averaged graphs were done in Radiance.

ANALYSIS

These temporal maps will ultimately be used as visual displays of data, intended to help architects make design decisions. Hence, it is important to confirm a visual and numerical similarity temporally averaged and the detailed reference case temporal maps. One must also ensure that the main visual features, those aspects of the map which, if lost, would cause the architect to misjudge the performance of the design, are not compromised by the averaging process. "Main features" typically refer to illuminance and variability over time of day or season, indications of sun penetration, or indications of weather patterns.

In addition to the visual comparison of these temporally averaged maps, pixel analyses were also done on greyscale versions; after dividing both averaged and Daysim temporal maps into map portions corresponding to the 56 annual divisions (figure 2), an average illuminance, corresponding to the average greyscale pixel brightness, was found for each of the 56 areas. The Mean Bias Error (MBE, between the averaged and Daysim maps), given in Equation 2, was then analyzed as a function of the 56 periods for each city. The Mean Bias Error is given as:

$$MBE = \frac{1}{N}\sum_{i=1}^{N}\frac{(P_{iA} - P_{iD})}{P_{iD}} \qquad (2)$$

where P_{iA} is the greyscale brightness of a pixel in the averaged Temporal Map and P_{iD} is the same pixel in the Daysim map. The error is summed and averaged over all pixels in a single period. These graphs allow one to analyze the similarity between the 56 period technique and the detailed data on a per temporal area basis. The Root Mean Square Error (RMSE) was not analyzed, because in this situation, a high standard deviation would not indicate a correlation failure. The method being presented is not intended to match the reference data perfectly, but to be a reasonable averaging process, in which case the effect of averaging peaks and troughs in the Daysim data would skew the RMSE artificially high and would not inform the appropriateness of the simplification methodology.

The one important exception to this reasoning is the inclusion of direct sun penetration. Direct sun can change the illuminance level at a point by orders of magnitude, and when architectural obstructions are present, it can appear or disappear rapidly. The inclusion of direct sun is discussed later in this paper.

To validate any proposal that heavily depends on weather and solar position, one needs to perform this validation for a group of locations representative of different climate types and latitudes. Ideally, a group of test locations would encompass a wide range of latitudes and a similarly wide spread of climate types. It would be heavy on those latitudes and climates most relevant to the majority of the world's population, which is distributed unevenly over the globe. The cities chosen should also be ones for which annual data is readily available.

The ten cities in Table 1 (listed in order of distance from the equator) represent both hemispheres, 5 continents, 5 climate types, a range of average sun hours per day, and a wide spread of latitudes. All have TMY2-type data (or similar) available on the Energy Plus website, and all are reasonably populous.

City	Lat.	Climate	Sun hrs
Singapore	1.2	Tropical	5.6
Addis Ababa	9.0	Highland	7
Bangkok	13.8	Tropical	7.2
Harare	-17.8	Hot Arid	8.3
Hong Kong	22.1	Warm Temperate	5.5
Phoenix	33.4	Hot Arid	11.1
Sydney	-33.8	Warm Temperate	6.7
Boston	42.3	Cool Temperate	7.4
London	51.5	Warm Temperate	4
St. Petersburg	59.9	Cool Temperate	4.5

Table 1: Ten cities used in outdoor comparison, chosen for their differences in latitude, sun hours, and climate. They are listed in order of distance from the Equator.

SIMULATION

Three cases were chosen for visual and pixel-based comparison, using a mixture of Radiance illuminance calculations and MATLAB processing. In each case, geometry, material, and photo-sensor point files were created for simulation in Radiance. A MATLAB file then processed TMY2 weather data and prepared Radiance batch files for simulation according to the methodology described above. (See Appendix for the Radiance parameters used in simulation.) Another MATLAB file processed the illuminance results output by Radiance and created a temporal map from the matrix of 56 values. For each case, a Daysim simulation was also performed on the same Radiance model files and in the same global locations. The illuminance data generated by Daysim, which represents one value every five minutes annually, was processed by another MATLAB program, which created a much more detailed reference case temporal map.

The first level of validation was performed with five unobstructed sensors under an open sky – one vertical sensor facing each cardinal direction and one horizontal sensor facing upwards. The purpose of this validation case is to compare the averaging method to the far more detailed Daysim data set without adding an architectural variable. The simulation was repeated for every location in Table 1.

The second validation case introduced a simple architectural model with large, continuous windows. A simple shoebox-like room was constructed and tested under Boston and Harare skies only (due to the greater simulation time required). The RADIANCE model

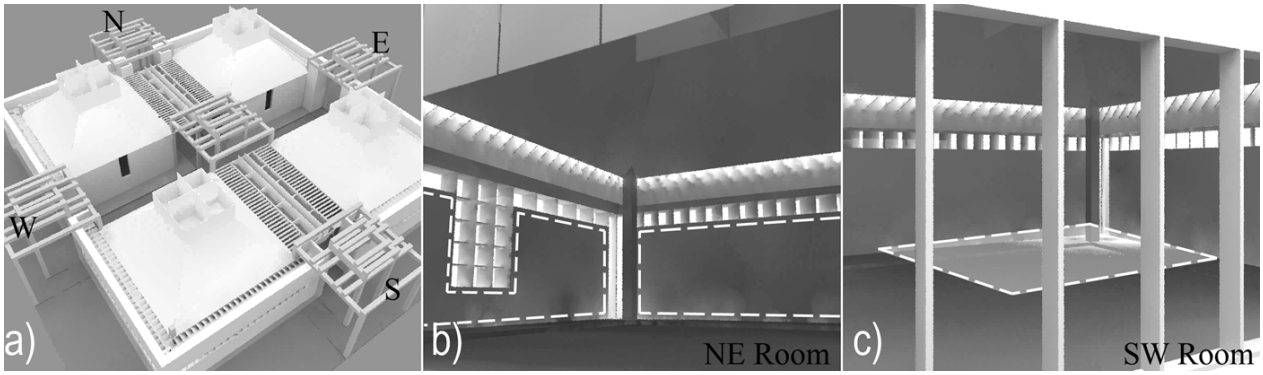

Figure 3: Museum design in Boston. a) Exterior rendering with compass directions indicated. b) Interior rendering of the Northeast room in which the dotted outline on the wall indicates area of interest. c) Interior rendering of the Southwest room in which area of interest is represented as a floating panel with a dotted outline.

consists of a rectangular room, 10m x 7.5m x 3m, in which the shorter facades face north and south. There is one south-facing window measuring 1.5 m tall and 5.5m wide with a head height of 2.5m, rendered without glass. The ceiling had a reflectance of 83%, the walls 65%, and the floor 5%. The idea behind this model was to restrict access to the sky but still provide a large, unbroken, direct connection. The shoebox model's sensor array is a 3x4 grid of 12 horizontal sensor points at the height of one meter to simulate a work plane.

The third validation case was based on a four-room museum design of much higher complexity and included features such as louvers, small windows, skylights, and lattices. The object of this level of validation was to see if the complex geometry changed the level of visual correlation between temporally averaged and Daysim temporal maps. Figure 3 shows an exterior (3a) and two interior shots (3b and c) of the museum model. The walls are around 70-75% reflective (diffuse), and the ceiling and skylight wells are about 80% reflective. The museum incorporates windows and angled louvered strips along all outer walls at eye level, around the roof edge, and hall and diffusing devices underneath the skylights. Two areas of interest were chosen in the museum: a horizontal area in the center of the southwest room at table height (1m), outlined in figure 3c and represented by 9 sensor points spaced 1.5m apart, and a vertical area along the north and east walls in the northeast room, outlined in figure 3b and represented by 10 sensor points in two rows of heights 0.65m and 2.5m. Averaged and Daysim temporal maps were produced for each sensor point in each area under Boston skies only.

RESULTS

The greatest visual difference between the averaged and Daysim temporal maps is effect of averaging. The Daysim maps, which have a resolution of 5 minutes, can show minute changes in weather and the "scan-line" striations of back-to-back clear and cloudy days, the result of which is a busy, almost fuzzy, Temporal Map. The Daysim map can show the exact illuminance at each sensor point at any time of the day or year, but on the smoother averaged map, general trends through time are also revealed clearly - and without what could be perceived as noise. In the first validation case, the visual effects of averaging are more pronounced in maps of cities in changeable climates – in other words, those cities which have a balanced number of clear and cloudy periods in quick succession with each other (Boston, Hong Kong, and Addis Ababa). Hot arid climates (Harare and Phoenix) tend towards more consistently sunny days, resulting mostly in a higher visual correlation between the two maps. Likewise, although Sydney and Bangkok have average sun hours that are closer to Boston's, the weather in those cities seems to change more slowly, causing less discrepancy. On the other extreme are very cloudy climates (London and St. Petersburg). The visual correlation between the averaged and Daysim maps for these cities is good, because the sunny "peaks" in the Daysim maps are so few and far between that they do not dominate, and are almost superfluous.

One definable discrepancy between the averaged and Daysim maps is systematic and more evident from a pixel analysis than from visual comparison. It was found that, in general, the data reduction process estimates illuminances that are lower than those produced by Daysim. Furthermore, there is a strong correlation between solar angle and this "underestimation". Since this problem is systematic and dependant on sun altitude, it is tempting to try to artificially correct for it, however, according to the study done by Littlefair [8], which found that the Perez All-Weather model *overestimated* sky luminances near the sun at low solar angles, it is not certain that the Daysim maps are the more accurate.

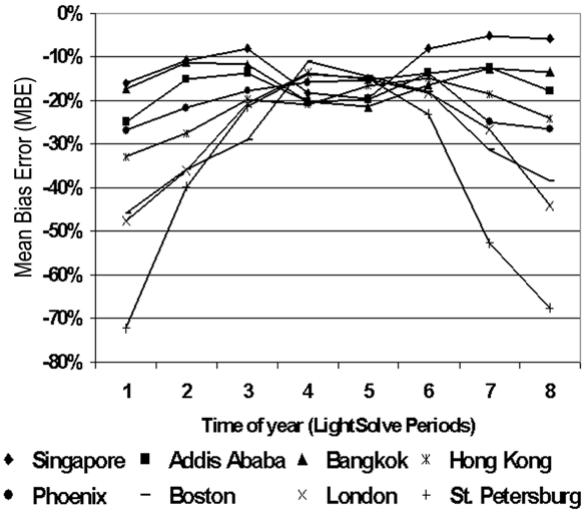

Figure 4: MBE between all south-facing averaged and Daysim temporal maps for northern-hemisphere cities as a function of time of year.

Figure 4 supports the phenomenon discovered by Littlefair; it shows the vertical, south-facing sensor MBE over the 8 annual averaging periods. During the summer, all cities have a 10-20% MBE, regardless of latitude. During the winter, however, the error clearly increases as latitudes get higher and solar angles get lower. Since the south-facing sensor is vertical and facing the sun, the sky-dome area most questioned by Littlefair, any differences would be emphasized. In short, there is a documentable difference between the averaged and Daysim results, but there is not enough evidence to support artificially correcting for a higher correlation between the two.

Having shown that the "unobstructed sky" averaged temporal maps are a reasonable correlation to those produced by Daysim, one must demonstrate that restricting the access to the sky (via architecture) does not seriously change this correlation. The resulting maps for the shoebox room, simulated for Boston and Harare, are visually and numerically quite similar to those for the south-facing unobstructed sensor (a more detailed explanation can be found in [13]). This is because the large, vertical window in the shoebox room gives a similar view of the sky as would be seen by that sensor. The indoor illuminance levels are much lower, and the MBE is on average about 10% less across the board, at some points tending slightly positive, rather than negative error. This is especially encouraging since most of the cases used to validate Daysim used indoor sensor points [2].

For general illuminance levels, the very same level of visual correlation was observed between averaged and Daysim temporal maps in the third model, the museum. One big difference, however, is that most of the sensor points never see the sky directly, or if they do, it is as tiny patches scattered over the hemisphere. Consequently, there are also small stripes or patches of direct sunlight moving around the rooms in each version of the design which were only intermittently captured using because of the small number of direct sun positions. To make matters more complex, Daysim is another program which somewhat limits the number of sun angles it simulates (see figure 1b), although Daysim does use a quick shadow-casting method to try to catch those smaller patches [14]. This results in Daysim catching more sun spots, but neither approach is immune to error in complex geometric situations.

Therefore, a zero-bounce sun penetration data set, calculated at 15 times per day and 80 times per year (1200 periods and 600 unique sun angles), is overlaid onto the general illuminance temporal maps where the "zero bounce" direct sun data exceeds the saturation level of the original map. The number 600 was considered sufficient in comparison with the Dynamic Daylight Simulation (DDS) scheme by Bourgeois, Reinhart, and Ward [15], since their 2305 direct daylight coefficient points are spread over the full sky dome, while these 600 sun angles are all concentrated within the actual angles of a location's specific sun path. Figure 5 is an example of this overlay.

In analyzing both the "shoebox" and "museum" models, it also became obvious that with so many sensor points, the number of temporal maps produced was becoming unwieldy. A method of compiling and displaying all data for a single area of interest was thus developed, resulting in graphs displaying not illuminance, but an area-based illuminance metric which corresponds to the percent of each area within the targeted illuminance range. Reversing Daysim's

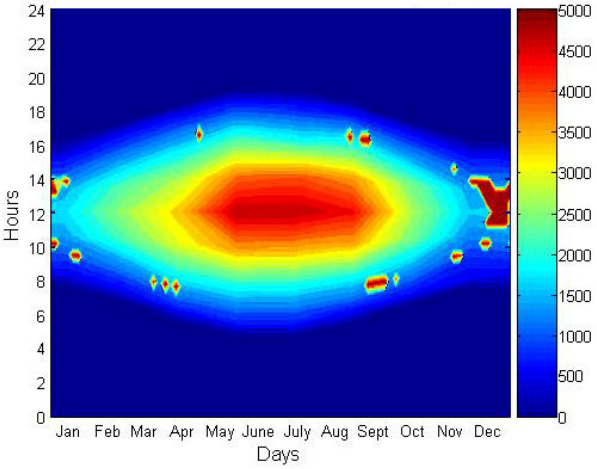

Figure 5: The illuminance temporal map from a horizontal sensor inside the museum. The small dark red spots indicate moments of direct sun hitting the sensor.

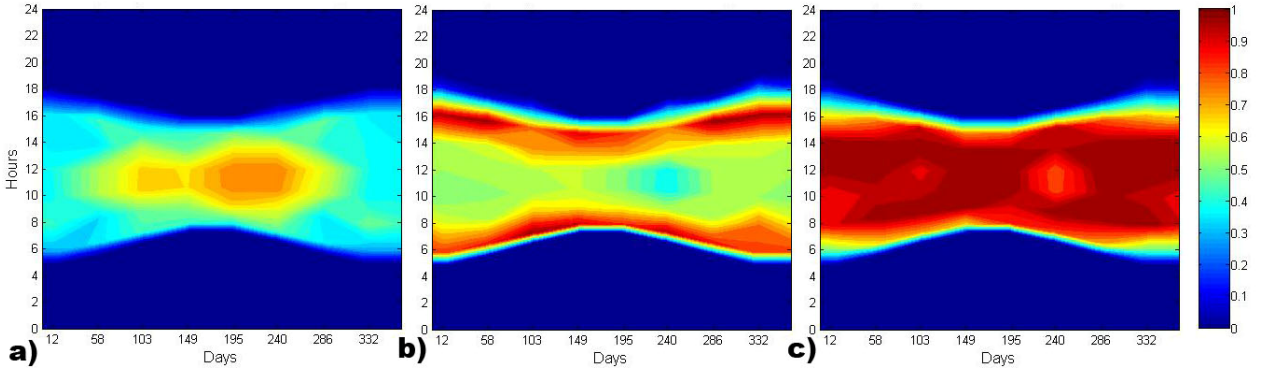

Figure 6: Three "percent-in-range" temporal maps representing the 3 iterations of the classroom mock design process ("a" is iteration 1, "b" is iteration 2, and "c" is iteration 3 as described below).

approach, the current illuminance metric displays the percent of the *area* which is within the desired range, and how it changes over *time*. In such a metric, the extra direct sun data would contribute to the bulk of "out of range" area.

APPLICATION TO A DESIGN PROCESS

The illuminance metric described above was used in an example of design decisions made with the help of temporal maps. This example walks through a mock design process for a classroom located in Sydney. For each design iteration, three temporal maps were produced showing the work plane percent "in range", "too low", and "too high". The desired range was 400-1500 lux with a "partial credit" buffer zone extending to 200 and 2000 lux from 7am to 4pm solar time during the academic year (February through November).

The first design iteration, whose performance is shown in Figure 6a, consisted of a north-facing unilateral punch window room with a flat roof and the spatial dimensions of the "shoebox" model (on an unobstructed plane). As a result, only 60%-75% of the work plane were in the desired range in winter and only 40%-50% in warmer months, while a significant portion of the space was too low throughout the year. Identical windows were then added to the south wall, which evened out the light but lowered the percent work plane in range to 50% (Figure 6b). Most of the out of range light measurements were too high, especially in the winter due to low sun angles, so the third design iteration decreased both north and south window areas. In addition, the north wall was made taller, the roof slanted, and the north window was raised, and bounded by an overhang and exterior light shelf. This was to ensure that while no direct sun penetrated the room, light would travel further into the space. (for more detailed descriptions, see [13].) These last changes made the classroom design 80%-100% in range all year long (Figure 6c).

This time-based design iterations sequence is particularly powerful to illustrate the usefulness and relevance of simplified temporal maps in a design process.

CONCLUSION AND OUTLOOK

The comparison models presented above show a strong visual and numerical correlation between temporal maps produced using the 56 annual periods method and those produced using detailed illuminance data extracted from the program Daysim. The result of averaging the illuminance over each area on the temporal map is that small details and the sense of immediate weather changeability are lost, while the changeability of performance on an annual scale is retained, and even made clearer. Furthermore, the overlay of high-frequency direct solar data compensates for the inability of a small number of annual periods (and thus a small sampling of possible sun angles) to capture the highly dynamic nature of direct solar irradiance.

Beyond illuminance, the authors hope to apply glare probability metrics and solar heat gain indicators to the temporal maps format. Similar methods of representing the annual performance of these metrics will be researched and will hopefully add to the future capabilities of a daylighting design tool.

While some components of this data processing and display methodology have been in existence for years, it is their unique combination that holds great promise in the capacity of informing architects' design decisions.

Climate-based, time-variable data are very valuable to the design process because they are able to reveal the nature of the environmental conditions in which a design performs well or poorly, to make visual comfort predictions, and because they encourage the designer to address the most important issues in daylighting with an annual perspective, such as building orientation,

position and size of openings, and shading strategies. This pre-processing of annual data and a proposal to link it with spatial renderings is an approach designed for a program named LightSolve. A work in progress, LightSolve would also incorporate interactive rendering optimization capabilities [16] and is described in further detail in [17].

APPENDIX

The parameters used in the RADIANCE simulations are as follows: -ab 7, -ar 128, -aa .1, -ad 2048, -as 256, -dp 4096, -ds .15, -dt .05, -dc .75, -dr 3, -ms 0.066, -sj 1, -st .01, -lr 12, -lw .0005, -I+, -h. The only exception to this was the museum model, which, for the sake of calculation time, used -ab 5, -ar 256, -aa .15, -ad 1024, -as 256, -dp 1024, -ds .15, -dt .1, -dc .75, -dr 3, -ms 0.1, -sj 1, -st .1, -lr 12, -lw .01, -I+, -h. (The increase in the resolution parameter is due to the vast decrease in size of the architectural elements.) All opaque materials were perfectly diffuse grey tones.

ACKNOWLEDGEMENTS

Siân Kleindienst and Dr. Marilyne Andersen were jointly supported by the Massachusetts Institute of Technology and the Boston Society of Architects (BSA). Dr. Magali Bodart was supported by the Belgian National Scientific Research Foundation for her contribution to LightSolve. The authors wish to thank Lu Yi for her museum design iterations and Dr Barbara Cutler for her continued involvement in the LightSolve project. They would also like to acknowledge Dr. Julie Dorsey for her guidance and advice during the project's conceptual stage.

REFERENCES

[1] Architectural Energy Corporation. (2006), 'Daylighting Metric Development Using Daylight Autonomy Calculations in the Sensor Placement Optimization Tool: Developmental Report and Case Studies', Prepared for CHPS Daylighting Committee

[2] Reinhart CF, Walkenhorst O. (2001), 'Validation of dynamic RADIANCE-based daylight simulations for a test office with external blinds', *Energy and Buildings*, 33(7) 683-697

[3] Mardaljevic J, Nabil A. (2006) 'The Useful Daylight Illuminance Paradigm: A Replacement for Daylight Factors', *Energy and Buildings*, 38(7) 905-913

[4] Reinhart CF, Mardaljevic J, Rogers Z. (2006), 'Dynamic Daylight Performance Metrics for Sustainable Building Design', *Leukos*, 3(1) 7-31

[5] Mardaljevic J. (2003) 'Precision Modeling of Parametrically Defined Solar Shading Systems: Pseudo-Changi', in 8th IBPSA conf., Eindhoven, Netherlands, August 11-14, 823-830

[6] Perez R, Michalsky J, Seals R. (1992), 'Modelling Sky Luminance Angular distribution for real sky conditions; Experimental evaluation of existing algorithms', Journal of the IES, 21(2) 84-92

[7] CIE. (1994), 'Spatial distribution of daylight – Luminance distributions of various reference skies', CIE Technical Report 110-1994

[8] Littlefair, PJ. (1994) 'A Comparison of Sky Luminance Models with Measured Data from Garston, United Kingdom', *Solar Energy*, 53(4) 315-322

[9] Perez R, Seals R, Michalsky J. (1993), 'All weather model for sky luminance distribution – preliminary configuration and validation', *Solar Energy*, 50 (3) 235-245

[10] Igawa N, Koga Y, Matsuzawa T, Nakamura H. (2004) 'Models of sky radiance distribution and sky luminance distribution', *Solar Energy*, 77(2) 137-157

[11] Marsh A. 'Ecotect: Thermal Analysis', Website maintained by Square One *research* Ltd; (last accessed Dec, 2007). http://squ1.com/ecotect/features/thermal

[12] Bund S, Do EYL. (2005), 'SPOT! Fetch Light Interactive navigable 3D visualization of direct sunlight', *Automation in Construction*, 14(2) 181-188

[13] Kleindienst S, Bodart M, Andersen M. (2008) 'Graphical Representation of Climate-Based Daylight Performance to Support Architectural Design', Submitted to *Leukos*

[14] Reinhart CF. (2005), 'Tutorial on the Use of Daysim/Radiance Simulations for Sustainable Design', NRC report, Ottawa, Canada

[15] Bourgeois D, Reinhart CF, Ward G. (2008), 'A Standard Daylight Coefficient Model for Dynamic Daylighting Simulations', *Building Research & Information*, 36(1) 68-82

[16] Cutler B, Sheng Y, Martin S, Glaser D, Andersen M. (2008), 'Interactive Selection of Optimal Fenestration Materials for Schematic Architectural Daylighting Design', *Automation in Construction* (in press)

[17] Andersen M, Kleindienst S, Yi L, Bodart M, Cutler B. (2008), 'Lightsolve – A New Approach for Intuitive Daylighting Performance Analysis and Optimization in Architectural Design'. Submitted to *Building Research & Information*